Derivation of an optimal directivity pattern for sweet spot widening in stereo sound reproduction

Josep A. Ródenas,[a] Ronald M. Aarts,[b] and A. J. E. M. Janssen
Philips Research Laboratories Eindhoven, Professor Holstlaan 4, NL-5656 AA Eindhoven, The Netherlands

(Received 12 March 2002; accepted for publication 27 September 2002)

In this paper the correction of the degradation of the stereophonic illusion during sound reproduction due to off-center listening is investigated. The main idea is that the directivity pattern of a loudspeaker array should have a well-defined shape such that a good stereo reproduction is achieved in a large listening area. Therefore, a mathematical description to derive an optimal directivity pattern ℓ_{opt} that achieves sweet spot widening in a large listening area for stereophonic sound applications is described. This optimal directivity pattern is based on parametrized time/intensity trading data coming from psycho-acoustic experiments within a wide listening area. After the study, the required digital FIR filters are determined by means of a least-squares optimization method for a given stereo base setup (two pair of drivers for the loudspeaker arrays and 2.5-m distance between loudspeakers), which radiate sound in a broad range of listening positions in accordance with the derived ℓ_{opt}. Informal listening tests have shown that the ℓ_{opt} worked as predicted by the theoretical simulations. They also demonstrated the correct central sound localization for speech and music for a number of listening positions. This application is referred to as ''*Position-Independent (PI) stereo.*'' © *2003 Acoustical Society of America.* [DOI: 10.1121/1.1527928]

PACS numbers: 43.38.Ar, 43.38.Hz, 43.38.Vk [SLE]

I. INTRODUCTION

This paper presents a mathematical derivation of a loudspeaker array to achieve correct localization for stereophonic sound reproduction in a wide listening area. An ideal stereophonic sound reproduction system is one which is capable of reconstructing the wavefront from a given sound scene in an exact form over a region in space occupied by the head of a listener. The use of two spatially separated loudspeakers imposes restrictions on the ability of stereophony to reconstruct the correct acoustic field so that a sharp image can be perceived. Such a system can provide a well-defined image for a centrally located listener mainly at low frequencies, depending on the geometrical displacement of the speakers relative to the listener (Blumlein, 1958).

The basis of stereophony is the ability to create *phantom sources*. It is known that the brain locates a monophonic signal originated from a single source by comparing the differences in the arrival time and intensity of that signal at each ear. If the same monophonic signal is played through two loudspeakers on either side of the listener, then the sound seems to appear from midway between the two loudspeakers since the traveling time of the signal arriving at each ear is the same. This is called a phantom (or virtual) source (Blumlein, 1958; Makita, 1962; Blauert, 1983). In the present work we will discuss how to enlarge the region within which the image remains reasonably free (Bauer, 1960; Crabbe, 1979). We consider only image localization in the horizontal plane since we are primarily interested in stereo sound reproduction.

In general, it can be stated that correct localization within a wide listening area is beneficial for all applications where a good stereophonic sound is required: audio, video, or car stereo. The idea of achieving an increase in the sweet spot area in a stereophonic setup has been recently introduced and studied at the Philips Research Labs in Eindhoven and the stereo sound system has been called ''*Position-Independent (PI) stereo* (Rodenas and Aarts, 2001a, b; Aarts, 1992). The main idea is that the directivity pattern of a loudspeaker array should have a well-defined shape such that a good stereo sound reproduction is achieved in a large listening area. Optimal digital filters are then designed and applied to individual drivers of linear loudspeaker arrays in order to obtain a directivity pattern of a specific shape. This shape has to be adapted to the time/intensity trading mechanism of the human auditory system via psycho-acoustic experiments within a wide listening area (Aarts, 1992).

The goal here is to derive an optimal directivity pattern ℓ_{opt} for the PI-stereo system, which is based on parametrized time/intensity trading data, and then to find, by means of an optimization process, the corresponding FIR filter coefficients that achieve this optimal directivity pattern. It has been proved that an optimal directivity pattern for a loudspeaker can be realized by using an array of drivers positioned at a specific distance from each other (Bauer, 1960; Kates, 1980; Davis, 1987). In our case we used the parametrized time/intensity trading data. Hence, achieving a practical design for PI-stereo sound reproduction, which is a pair of loudspeaker cabinets each equipped with a pair of drivers, which are separated at a given distance to achieve two frequency ranges (high and mid), so as to obtain the desired optimal directivity pattern.

We start first, in Sec. II, describing the limitation of having a sweet spot and the need to improve the stereo-

[a]Currently with Hewlett-Packard, Avda. Graells 501, 08190 Sant Cugat, Spain. Electronic mail: josep_rodenas@hp.com
[b]Author to whom correspondence should be addressed. Electronic mail: ronald.m.aarts@philips.com

phonic sound reproduction system. Section III describes the human auditory localization, since it is the sound field as perceived by the listener that determines the apparent phantom source. In Sec. IV we introduce briefly the PI-stereo system. Then, in Sec. V, we present the mathematical description to obtain the optimal directivity pattern that gives the best localization performance. We also describe the optimization method to derive the required FIR filter coefficients to drive the loudspeaker cabinets. Later, in Sec. VI, we present the time, frequency, and polar responses of the optimal FIR filters for a practical implementation of two drivers for the loudspeaker arrays. In Sec. VII we present the measured directivity patterns in an anechoic room. Some preliminary listening tests and discussion on the performance of the implemented PI-stereo system will be described in Sec. VIII. Finally, the main conclusions will be summarized in Sec. IX.

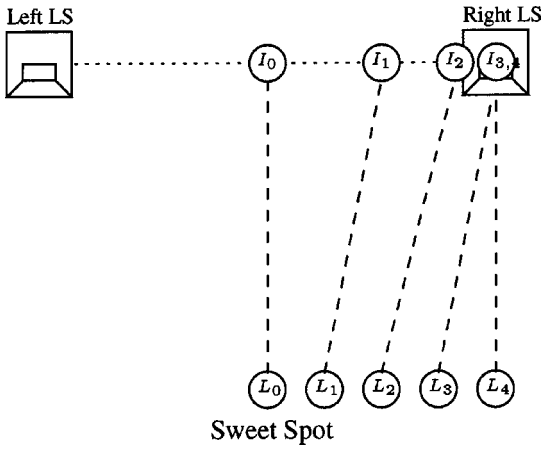

FIG. 1. Conventional arrangement of loudspeakers exhibiting the apparent motion of the phantom sound image I_n for several listener positions L_n.

II. SWEET SPOT LIMITATION

Generally it is considered as a serious artifact of the traditional stereo system that the stereophonic illusion works only in a limited region. Optimum stereo perception only occurs if the listener is placed exactly in the median plane between the two loudspeakers (*sweet spot*).

One reason that there is a sweet spot is that in two-loudspeaker reproduction, the signals at the listener's ears are formed by the interference of acoustic waves emanating from the loudspeakers. With two loudspeakers, the field can be controlled precisely at only two points (unless unusual acoustical conditions exist, such as the presence of resonant structures). For the present application, those points are at the listener's ears. If the listener moves his head so that the ears are no longer at the designated positions, sound image distortion will appear, caused by unintended signals created by unanticipated interference. Primary causes of the changing interference are differing times of arrival due to differing loudspeaker listener distances, amplitude variations of the impinging waves due to these same varying distances (aggravated by the listener sitting close to the loudspeakers), and uncompensated secondary reflections (improved by the listener sitting close to the loudspeakers) (Leakey, 1960; Jordan, 1971; Lipshitz, 1986).

These problems are illustrated with one example as shown in Fig. 1. The localization performance of a listener using a conventional stereo setup can be quite poor for a listener positioned off-center. Consider a center-front soloist, or, equivalently, assume that the two loudspeakers are radiating exactly the same sound pressure precisely in phase. When the listener is equidistant from the two loudspeakers, the apparent phantom source is perceived to be centered between the loudspeakers. This is illustrated in the figure, where L_0 is the centered listener and I_0 is the intended centered image. As the listener moves to the right, the perceived image also moves to the right. This is shown by the succession of perceived images I_1 through I_4, which correspond to listener positions L_1 through L_4. Finally, at listener position L_4, what is intended to be a centered image is perceived instead as coming from the right loudspeaker.

Thus, if the head is moved laterally, the sound rapidly seems to come from the nearest loudspeaker only. As pointed out, this is mainly because of two additional effects: the intensity of the nearest loudspeaker at the listener's head is highest, and its wavefront arrives earlier (law of the first wavefront or *precedence effect*) (Blauert, 1983).

III. AUDITORY LOCALIZATION

By comparing the signals at the ears, the brain is thought to derive two primary psycho-acoustic cues that determine the perceived horizontal position of a sound source. These broad mechanisms involve the detection of timing or phase differences between the ears (*interaural time differences* or ITDs), and of amplitude or spectral differences between the ears (*interaural intensity difference* or IIDs), which explains all major phenomena of frequency-dependent localization (Stevens and Newman, 1936; Leakey, 1959; Franssen, 1960). They are caused by the wave propagation time difference (primarily below 1.5 kHz) and the shadowing effect of the head (primarily above 1.5 kHz), respectively.

The binaural system is mainly sensitive to IID cues for frequencies above about 500 Hz. IID cues become large and reliable for frequencies above 3000 Hz, making IID cues most effective at high frequencies. In contrast, the binaural system is capable of using ITD cues only at low frequencies, below about 1500 Hz (Kates, 1980).

We will use these binaural differences by employing the phenomena of *time-intensity trading* (the ability to compensate for a left or right bias in the time of arrival by introducing a counterbias in amplitude) (Franssen, 1960; Blauert, 1983; Aarts, 1992). As the listener gets closer to one loudspeaker and sounds arrives sooner, sound from the far loudspeaker should become louder by a certain amount. This means that the loudspeaker should radiate more loudly in some directions than in others. In theory, if the pattern of level as a function of angle is chosen properly, the imaging will be rendered stable for listening positions in a wide listening area. This is actually the goal of the PI-stereo system, and therefore we are now in a position to introduce the basis of the PI-stereo sound system.

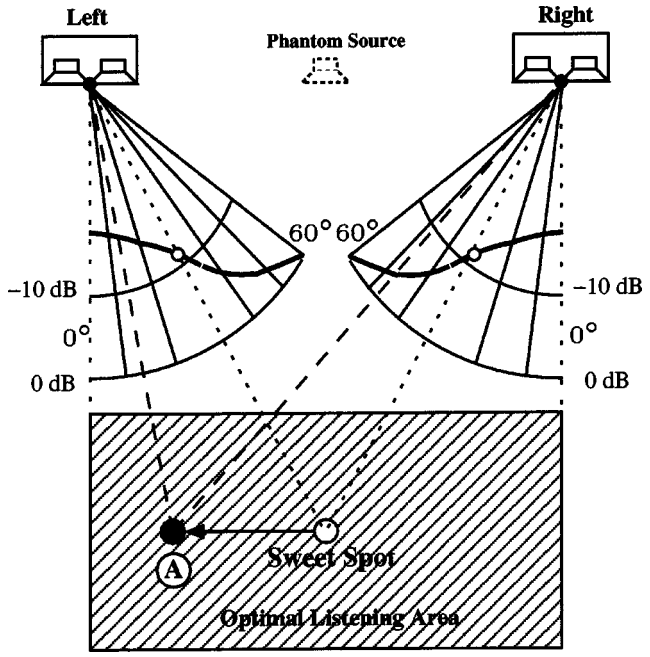

FIG. 2. Optimal listening area for PI-stereo sound reproduction.

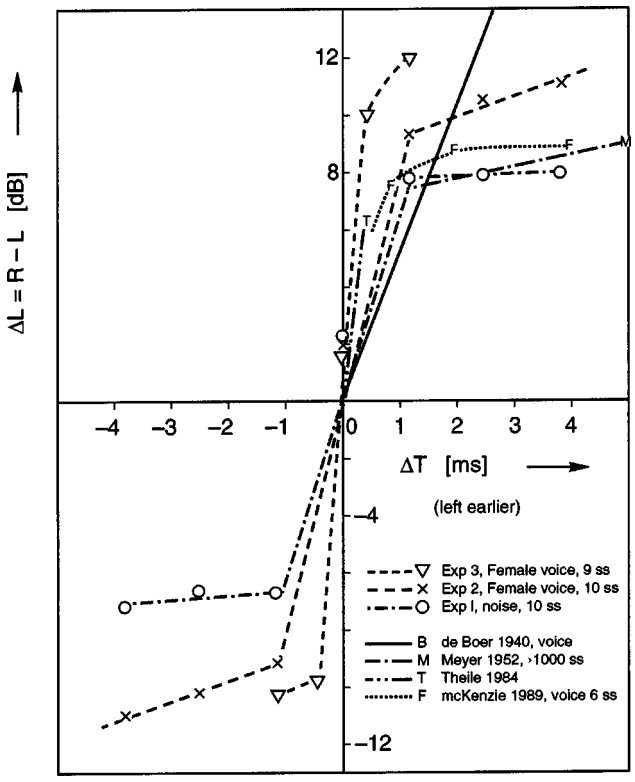

FIG. 3. Time/intensity trading results from the experiments in comparison with other experiments from the literature [after Aarts (1992)].

IV. THE POSITION-INDEPENDENT STEREO SYSTEM

The current PI-stereo system is basically composed of two loudspeaker arrays, each fitted into a single cabinet, together with an optimal directivity pattern which has been designed such that a good stereo sound reproduction is achieved in a large listening area (Rodenas and Aarts, 2001a, b). A standard listening setup for PI-stereo sound reproduction is shown in Fig. 2.

The main idea here is the following: if the listener moves to the left position (A), the sound intensity from the right loudspeaker increases at the listener's position, while that of the left loudspeaker decreases in such a way that this intensity difference compensates the time arrival difference from both loudspeakers. Thus, the phantom source remains in the middle. This can also be seen as a sort of automatic balance control depending on the position of the listener. However, the PI-stereo system we propose here is passive and does not depend on the position of the listener.

In order to calculate the required directivity pattern, that is the amount of intensity level compensation required for the loudspeakers, listening tests in an anechoic room were conducted (Aarts, 1992). During these tests, the differences in intensity levels between right and left loudspeakers needed to obtain a central sound image for several listening positions were measured (see Fig. 3). From these experiments, which were done by using broadband signals, the required differences for the sound-pressure values at different angles for the loudspeakers were determined and thus the time/intensity trading data.

In the next section, we will introduce the approach consisting of a mathematical derivation, which is based on parametrized time/intensity trading plots, to derive an optimal directivity pattern ℓ_{opt} for the loudspeaker array and, consequently, to obtain the optimal FIR filter coefficients for a specific stereo sound reproduction setup consisting of two drivers for each of the loudspeaker arrays that are separated by a distance of 2.5 m.

V. MATHEMATICAL DERIVATION

A. Definition of the problem

We wish to find the optimal directivity pattern ℓ_{opt} that achieves a correct sound localization (robust PI-stereo effect) in a wide listening area for a specific stereo base distance. The PI-stereo problem is considered to be symmetrical and it can be described in the setup shown in Fig. 4.

The sound pressures p_L and p_R at a given point $s=(r,\theta)$ due to the left and right loudspeaker arrays, respectively, are given by

$$p_L(\Omega_L,\theta,r_L)=\frac{e^{-i\omega r_L/c}}{r_L}\sum_{m=-M}^{M}x_{L,m}e^{im\Omega_L}, \tag{1}$$

$$p_R(\Omega_R,\theta,r_R)=\frac{e^{-i\omega r_R/c}}{r_R}\sum_{m=-M}^{M}x_{R,m}e^{im\Omega_R}, \tag{2}$$

where θ is the angle of observation, d is the distance between the drivers in each loudspeaker array (1 cm$<d<$10 cm), D is the distance between the centers of the two loudspeaker arrays (1 m$<D<$5 m), $\Omega_L=\omega d\sin\varphi_L/c$ with $0<\varphi_L<\pi/4$ and $\Omega_R=\omega d\sin\varphi_R/c$ with $0<\varphi_R<\pi/4$, ω is the angular frequency of the sound with $\pi c/10d\leqslant\omega\leqslant\pi c/d$, r is the distance from the origin to the observation point $s=(r,\theta)$, r_L is the distance from the center of the left loudspeaker array to s and r_R is the distance from the center of the right loudspeaker array to s, c is the velocity of sound ($c=343$ m/s), $x_{L,m}$ is the complex coefficient for the mth

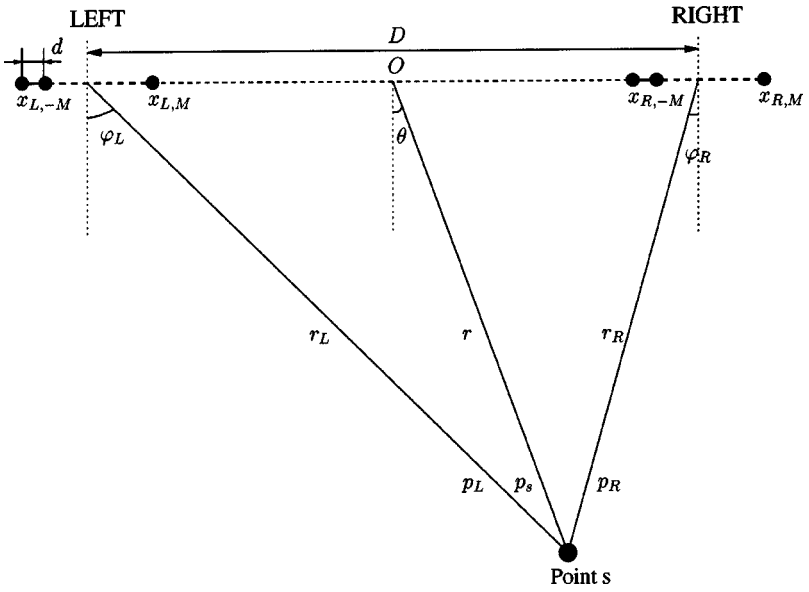

FIG. 4. Setup for the mathematical derivation of robust PI-stereo.

driver of the left loudspeaker array and $x_{R,m}$ is the complex coefficient for the mth driver of the right loudspeaker array with $|x_{\{R\}}^{\{L\}},_m| \leqslant 1$, $x \in \mathbf{C}$, and $N=2M+1$ is the number of drivers in each loudspeaker array, with the constraints $d \ll r$ and $d \ll D$. In this case N is odd; however, for the case N is even we arrive at similar formulas and we will use $N=2$ as an example in Sec. VII.

The sound pressure at point s due to both loudspeaker arrays is

$$p_s = p_L + p_R . \tag{3}$$

We want to determine $x_{\{R\}}^{\{L\}},_m(\omega)$ such that

$$\int_A \epsilon^2(r,\theta,x_L,x_R) w(r,\theta) dA \tag{4}$$

is minimal, where A is the listening area, $w(r,\theta)$ is a weight function, the error

$$\epsilon = \Delta L - f(\Delta T), \tag{5}$$

and $\Delta L = 20 \log|p_R/p_L|$. The parametrized function $f(\Delta L)$ is depicted in Fig. 5 and it is based on time/intensity trading experiments as given in Fig. 3. This function has the following form:

$$f(\Delta T) = \begin{cases} \alpha_1 \Delta T & \text{for } 0 \leqslant \Delta T \leqslant t_1 \\ \alpha_2(\Delta T - t_1) + f(t_1) & \text{for } \Delta T > t_1 \end{cases} , \tag{6}$$

where $f(-\Delta T) = -f(\Delta T)$, $\Delta T = (r_R - r_L)/c$, and t_1 is in ms, α_1 and α_2 are in dB/ms.

B. Solution of the problem

We fix $\omega \in [\pi c/10d, \pi c/d]$. When solving the described problem we consider the geometrical description shown in Fig. 6. We should then deal with the symmetrical setup, in which a given sound pressure F is

$$F(r_L,\varphi_L) = p_L(\Omega,\theta,r) \quad \text{and} \quad F(r_R,\varphi_R) = p_R(\Omega,\theta,r), \tag{7}$$

where

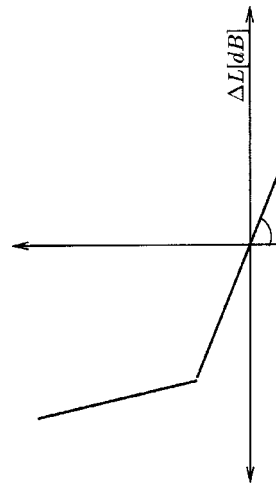

FIG. 5. Parametrization of the time/intensity trading data.

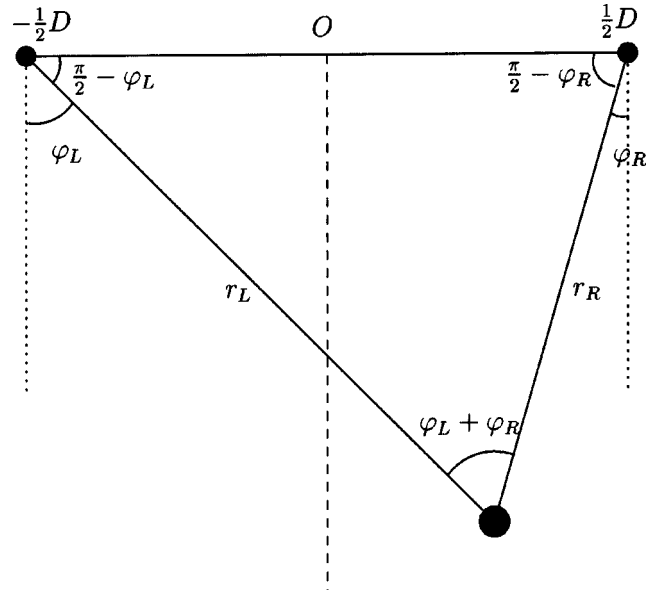

FIG. 6. Trigonometrical geometry for solving the mathematical derivation.

$$F(r,\varphi)=\frac{e^{-i\omega r/c}}{r}\sum_m x_m e^{(im\omega d\ \sin\ \varphi)/c}. \tag{8}$$

We set

$$G(z)=\left|\sum_m x_m e^{(imzd)/c}\right|, \tag{9}$$

so that

$$|F(r,\varphi)|=\frac{G(\omega\ \sin\ \varphi)}{r}. \tag{10}$$

The distance term r in Eq. (10) compensates for the intensity difference causes by the corresponding pathlength to the observation point s. These distances are already incorporated in the experimental data on the time/intensity trading. Since we are interested in finding only the optimal directivity pattern at the left and right loudspeaker arrays, we should not now include this term in the derivation. Then, Eq. (10) becomes:

$$|F(\varphi)|=G(\omega\ \sin\ \varphi). \tag{11}$$

Therefore, as previously described in Eq. (5), our objective is to minimize the average value of

$$\epsilon^2(\varphi_L,\varphi_R)=\left|20\log\left|\frac{F(\varphi_R)}{F(\varphi_L)}\right|-f\left(\frac{r_R-r_L}{c}\right)\right|^2, \tag{12}$$

while maximizing the total average power. Note that the right-hand side of Eq. (12) is invariant with respect to multiplication of F by a constant. Hence, one should aim to find an F that minimizes Eq. (12) such that $\max_m|x_m|=1$ in order to maximize power.

We note that the error ϵ in Eq. (12) is just a function of φ_L, φ_R, and the distances r_R and r_L being determined by φ_L and φ_R. We can eliminate r_R and r_L by expressing them in terms of φ_L and φ_R by using the *sine rule* as follows (see also Fig. 6):

$$\frac{\sin(\pi/2-\varphi_L)}{r_R}=\frac{\sin(\pi/2-\varphi_R)}{r_L}=\frac{\sin(\varphi_L+\varphi_R)}{D}, \tag{13}$$

so that

$$r_L=\frac{D\ \cos\ \varphi_R}{\sin(\varphi_L+\varphi_R)};\quad r_R=\frac{D\ \cos\ \varphi_L}{\sin(\varphi_L+\varphi_R)}. \tag{14}$$

Consequently, we have

$$r_R-r_L=\frac{D(\cos\ \varphi_L-\cos\ \varphi_R)}{\sin(\varphi_L+\varphi_R)}=\frac{D\ \sin 1/2(\varphi_R-\varphi_L)}{\cos 1/2(\varphi_R+\varphi_L)}. \tag{15}$$

Hence, the error ϵ is given by

$$\epsilon^2(\varphi_L,\varphi_R)=\left|20\log G(\omega\ \sin\ \varphi_R)-20\log G(\omega\ \sin\ \varphi_L)-f\left(\frac{D\ \sin 1/2(\varphi_R-\varphi_L)}{c\ \cos 1/2(\varphi_R+\varphi_L)}\right)\right|^2. \tag{16}$$

We now let

$$\ell(\varphi)=20\log G(\omega\ \sin\ \varphi), \tag{17}$$

and

$$h(\varphi,\psi)=f\left(\frac{D\ \sin 1/2(\varphi-\psi)}{c\ \cos 1/2(\varphi+\psi)}\right) \tag{18}$$

for $0\leqslant\varphi,\ \psi\leqslant\pi/2$. Since f is odd, we have

$$h(\varphi,\psi)=-h(\psi,\varphi). \tag{19}$$

We then seek to minimize the average value of

$$|\ell(\varphi)-\ell(\psi)-h(\varphi,\psi)|^2,\quad \text{with}\ \ \varphi=\varphi_R,\psi=\varphi_L \tag{20}$$

over all square integrable functions ℓ (with respect to the weight function w). Having found this ℓ_{opt}, we must find the coefficients x_m as in Eq. (9) such that the average value of

$$|\ell(\varphi)-20\log G(\omega\ \sin\ \varphi)|^2 \tag{21}$$

is minimal.

In order to minimize the average value of Eq. (20), we introduce a weight function of the form

$$W(\varphi,\psi)=w(\varphi)w(\psi),\quad 0\leqslant\varphi,\psi\leqslant\pi/2 \tag{22}$$

with $w(\varphi)$ a bounded, non-negative function of $\varphi\in[0,\pi/2]$, and we seek to minimize

$$\int_0^{\pi/2}\int_0^{\pi/2}|\ell(\varphi)-\ell(\psi)-h(\varphi,\psi)|^2W(\varphi,\psi)d\varphi\ d\psi \tag{23}$$

over all square integrable functions ℓ. The restriction to W of the particular form in Eq. (22) is made to facilitate the developments in the Appendix. Since the functional, as given by Eq. (23), depends on ℓ through the difference $\ell(\varphi)-\ell(\psi)$, so that adding a constant to ℓ yields the same value, we require that

$$\int_0^{\pi/2}\ell(\varphi)w(\varphi)d\varphi=0. \tag{24}$$

In the Appendix we show that the minimizing $\ell=\ell_{\text{opt}}$ is given by

$$\ell_{\text{opt}}(\varphi)=\frac{1}{C}\int_0^{\pi/2}h(\varphi,\psi)w(\psi)d\psi, \tag{25}$$

where

$$C=\int_0^{\pi/2}w(\varphi)d\varphi. \tag{26}$$

Furthermore, we show in the Appendix that the evaluation of the integral on the right-hand side of Eq. (25) with h given in Eq. (18) can be done according to

$$\int_0^{\pi/2}h(\varphi,\psi)w(\psi)d\psi=2\cos\ \varphi\int_{-1}^{\tan 1/2\ \varphi}f\left(\frac{D}{c}x\right)\times\frac{w(\varphi-\arctan(x\ \cos\ \varphi/(1-x\ \sin\ \varphi)))}{1-2x\ \sin\ \varphi+x^2}dx, \tag{27}$$

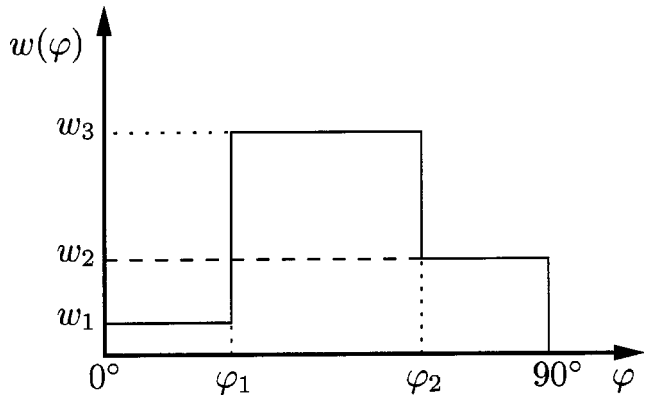

FIG. 7. Weight function to emphasize the region over which the optimization is carried out.

where $0 \leqslant \varphi \leqslant \pi/2$. With f a piecewise linear function as in Eq. (6) and w a piecewise constant function as, for instance, in Fig. 7, the evaluation of ℓ_{opt} reduces to applying the appropriate analytic formulas for integrals involving low-degree rational integrands.

The function ℓ_{opt} found above is, in general, not of the special form as in Eq. (17) with a G as given in Eq. (9) where we use the coefficients x_m. Hence, we describe the approach to derive the x_m used in Eq. (9) in the next section.

C. Optimization to find the optimal filter coefficients x_m

To find the required FIR filter coefficients x_m we use a *least-squares optimization* method (Marquardt, 1963; Dennis, 1977) such that

$$2C \int_0^{\pi/2} \left| 20 \log \left| \sum_m \hat{x}_m(\omega) e^{(im\omega \sin \varphi)/c} \right| - \ell_{\text{opt}}(\varphi) \right|^2 w(\varphi) d\varphi \tag{28}$$

is minimal. Note here that the coefficients $\hat{x}_m(\omega)$ depend on the frequency ω. The optimal x_m are then found as

$$x_m = S\hat{x}_m, \tag{29}$$

where m is the driver index and the scaling constant S is such that $\max_{m \in \mathbf{R}} |x_{m,\text{opt}}| = 1$.

D. Simulation results

We show here some simulations for the optimal directivity pattern ℓ_{opt} obtained from the computation of Eq. (25). Figure 7 shows the type of weight function used in this study. This function depends on three weights (w_1, w_2, and w_3) at given angles (φ_1 and φ_2). In this case we chose: $w_1 = w_2 = 0$ and $w_3 = 1$ at angles $\varphi_1 = 24.35°$ and $\varphi_2 = 37.25°$. This choice emphasizes the middle angles (in relation to the working region 0°–60°) over the extreme angles.

Figure 8 shows the results from the simulations for ℓ_{opt} for several stereo base distances going from 1 to 2.5 m for angles in the working region (0°–60°) for PI-stereo. The parametrized time/intensity trading parameters have been obtained from the data plots (for stereo base distances of 2.5 and 1 m) coming from Aarts (1992), and for the remaining

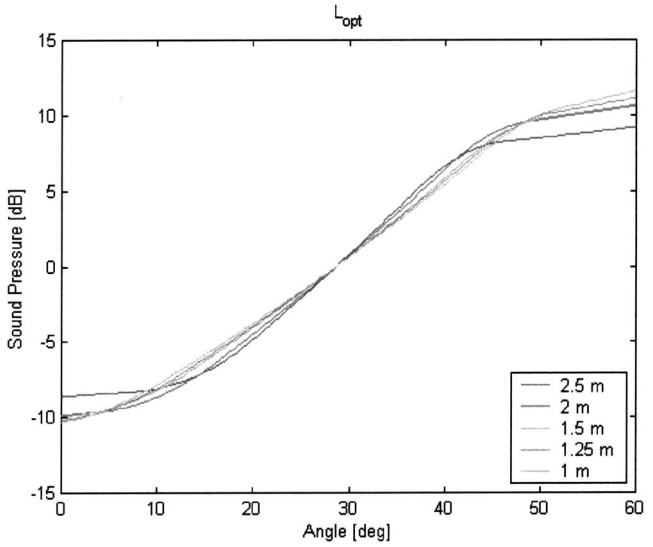

FIG. 8. ℓ_{opt}'s in the working region (0°–60°) for several stereo base distances.

distances, some approximation curves were derived to estimate the parameters. The stereo base distances used for the simulations are presented in Table I.

Figure 9 shows the resulting time/intensity trading plots obtained from the estimated ℓ_{opt}'s for the two stereo base distances (1 and 2.5 m) compared with the time/intensity trading plots given by Aarts (1992). It can be seen that for very small time differences (that is, for middle angles) the approximation is quite good; however, for larger time differences the approximation becomes slightly worse. The reason for these approximation errors in the time/intensity trading data comes basically from the fact that we are trying to achieve an optimal directivity pattern for a wide area, thus giving an approximate optimal directivity pattern at all positions in the listening area. Since we have applied the weight function at the intermediate angles, the approximation in this region is better.

VI. OPTIMAL FIR FILTER RESPONSES

We have used the optimization method described in Sec. V C to obtain the optimal FIR filters x_m which achieve the derived optimal directivity pattern ℓ_{opt} using MATLAB. We used the ℓ_{opt} previously found for a 2.5-m stereo base distance. We also used $N = 2$ as a number of drivers for the left and right loudspeaker arrays (we will refer to these drivers from now on as A and B). It is important to note here that

TABLE I. Stereo base distances D and parametrized time/intensity trading parameters (α_1, α_2, and t_1) for the function given in Eq. (6) used in the simulation of ℓ_{opt}.

	Parametrized $f(\Delta T)$		
Distance (m)	α_1 (dB/ms)	α_2 (dB/ms)	t_1 (ms)
1	15.62	3.54	0.64
1.25	13	2.27	0.75
1.5	11.17	1.55	0.85
2	9.25	1.16	1
2.5	8	0.7	1

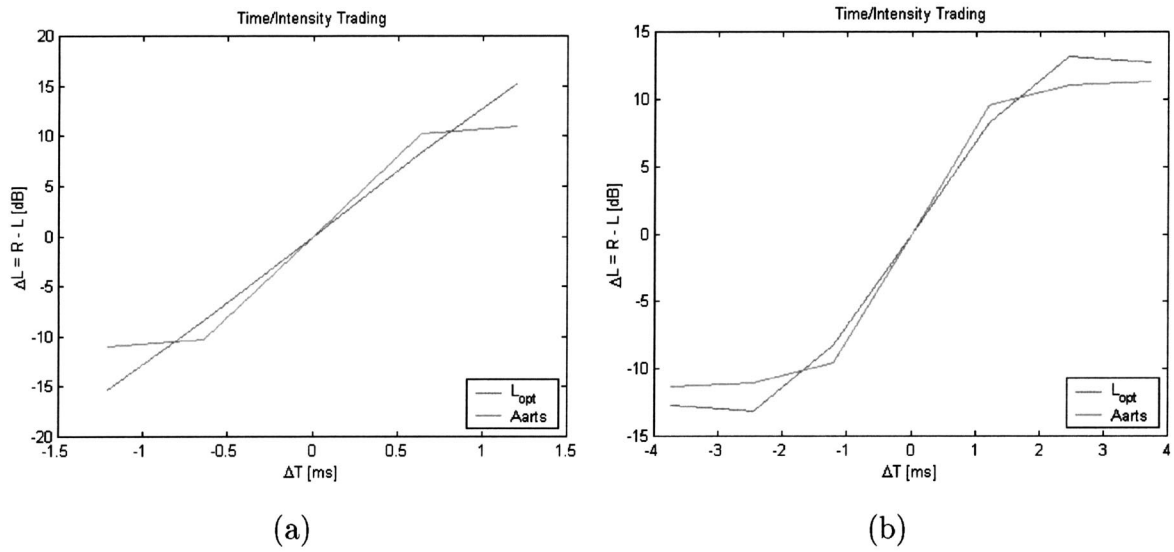

FIG. 9. Time/intensity trading approximations for the parametrized time/intensity trading plot coming from the ℓ_{opt} compared with the time/intensity trading plot given by Aarts (1992). (a) Stereo base of 1 m. (b) Stereo base of 2.5 m.

since the processing of PI-stereo is split into two frequency bands (200–2000 Hz for midrange and 2000–12 000 Hz for high range), the optimization has been computed for these two frequency ranges (see Fig. 10).

Figure 11 shows the results for the estimated FIR filters for 40 coefficients. Figure 11(a) shows the impulse and frequency responses of the *A* and *B* drivers for the midrange filters, and Fig. 11(b) shows the responses of the *A* and *B* drivers for the high-range filters. We can see that the impulse responses of filters *A* and *B* are odd-symmetric; thus, the magnitudes of the transfer functions are the same, only the phase differs. This can be observed from the frequency responses of the filters. We notice that the filters generally have a low-pass behavior.

Figure 12 presents the theoretical sound pressures and the obtained polar plots when using the estimated FIR filter coefficients. Figure 12(a) shows the plots for the midrange and Fig. 12(b) for the high range. It can be easily observed that the final approximation error to the desired optimal directivity pattern ℓ_{opt} is quite large. This is due to the fact that in our case we are limited to the use of only two drivers to achieve the desired ℓ_{opt} which is obviously not good enough. Indeed, the more drivers (thus filters) we use in the optimization method, the better the approximation we get to the ℓ_{opt} in the directivity pattern simulation (see Fig. 13).

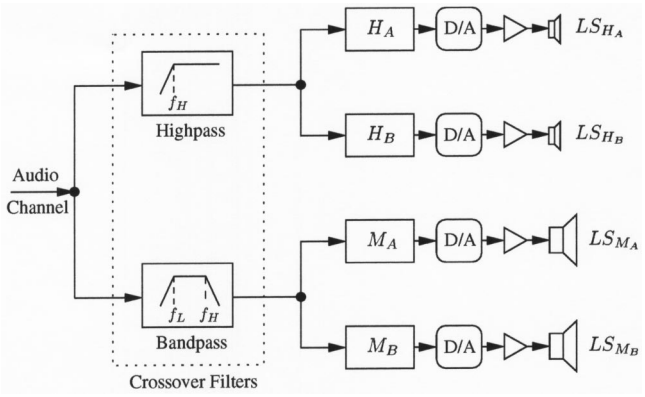

FIG. 10. A schematic block diagram of one array for the processing of one of the audio channels. The frequency range splitting is achieved by means of crossover filters. Filters H_A and H_B for the high-frequency range and filters M_A and M_B for the midfrequency range are obtained by the proposed method. These filters drive the two arrays of loudspeakers, LS_{H_A}, LS_{H_B} and LS_{M_A}, LS_{M_A}.

VII. MEASUREMENT RESULTS OF THE DIRECTIVITY PATTERNS

We have measured the impulse responses at stated angles of the PI-stereo system using the computed FIR filters. The impulse response measurements were done with a system for acoustical measurements which is based on a turntable for loudspeaker rotation and on a maximum-length sequence (MLS) measurement system.

The PI-stereo cabinet to be measured was placed on the turntable facing a microphone (1/2-in. 4133 free-field B&K). Impulse response measurements were done every 5° so that a total of 72 measurements was realized in one revolution.

Figure 14 shows the measured directivity patterns normalized at half of the working regions for PI-stereo (i.e., 30°) for the right response PI-stereo cabinet in an anechoic room at different frequencies. For comparison purposes, we should focus our attention on the working region for PI-stereo for angles going from 0° to 60°. Although the intent of the PI-stereo implementation of this paper is to generate frequency-independent directivity patterns, it is clear that there are significant deviations at higher frequencies.

VIII. INFORMAL LISTENING TESTS AND DISCUSSION

We have tested the PI-stereo system for a distance of around 2.5-m separation between the left and right PI-stereo cabinets. A listening room was used to study the influence of room boundaries, and despite room reflections, the PI-stereo effect remained.

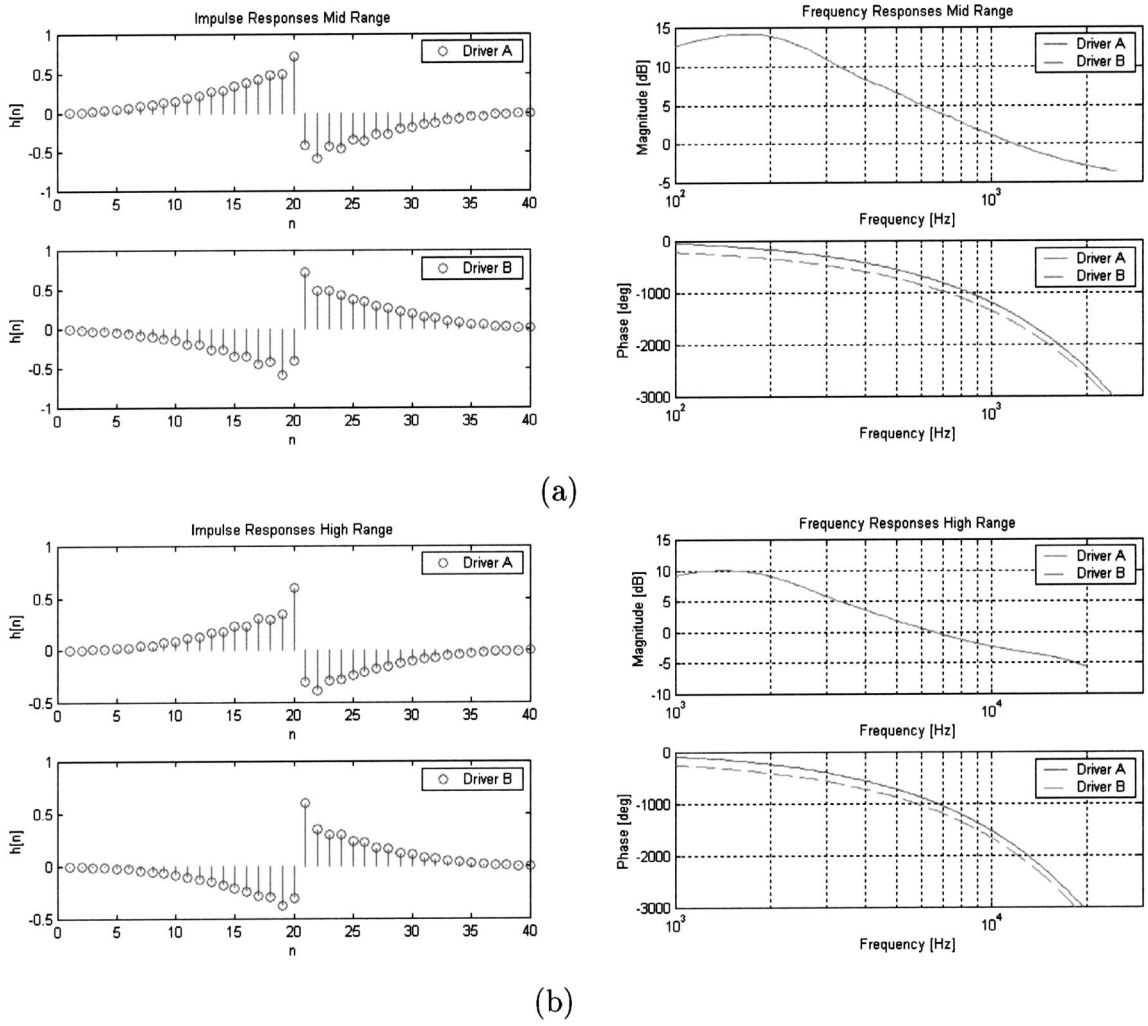

FIG. 11. Impulse and frequency responses of the 40-tap FIR filters. (a) Midrange. (b) High range.

A group of experienced listeners (7 subjects) tested the PI-stereo system in comparison with normal stereo at different on- and off-axis listening positions. Some of the parameters considered for comparison were: sound localization, apparent source width (ASW), coloration, and loudness.

Both normal stereo and PI-stereo were reproduced by the same loudspeaker cabinets, so there was no shift in the stereo image at the sweet spot. Some informal listening tests were undertaken to investigate the sound localization performance and robustness of the obtained optimal directivity pattern ℓ_{opt} and the associated FIR filters. From the experiments, it was observed that the influence of the stereo base distance was not critical to notice the PI-stereo effect (it only became slightly overdone, for narrower distances, or underdone for wider distances).

The listener's observations showed that the PI-stereo system worked as predicted by the simulation plots (see Sec. VI). Correct central sound localization for speech and music was demonstrated for a number of on- and off-axis listening positions. The difference between normal stereo and PI-stereo at the sweet spot was very modest. The stereo sound sensation, in particular the placement of central voices, was independent of the listening position within a large area. This central placement of voices was specially appreciated when listening to the PI-stereo system for a TV setup. When listening to normal stereo at lateral positions, listeners experienced an annoying spatial distortion in that the sound did not come from the same position as the TV image. The differences between normal stereo and PI-stereo depends somewhat on the type of the music recording; however, for PI-stereo the sound was well localized, coming from the same location as the TV image.

In conclusion, we can summarize the main results obtained from the listening tests

(i) Robust sound image in terms of sound localization;
(ii) Well-localized and clear centered phantom source; and
(iii) Better spatial images at lateral positions.

IX. CONCLUSIONS

We have introduced a new position-independent system for stereophonic sound reproduction ensuring correct sound localization in a large listening area. A mathematical derivation to achieve an optimal directivity pattern which offers a more robust and natural high-quality stereo sound in a large

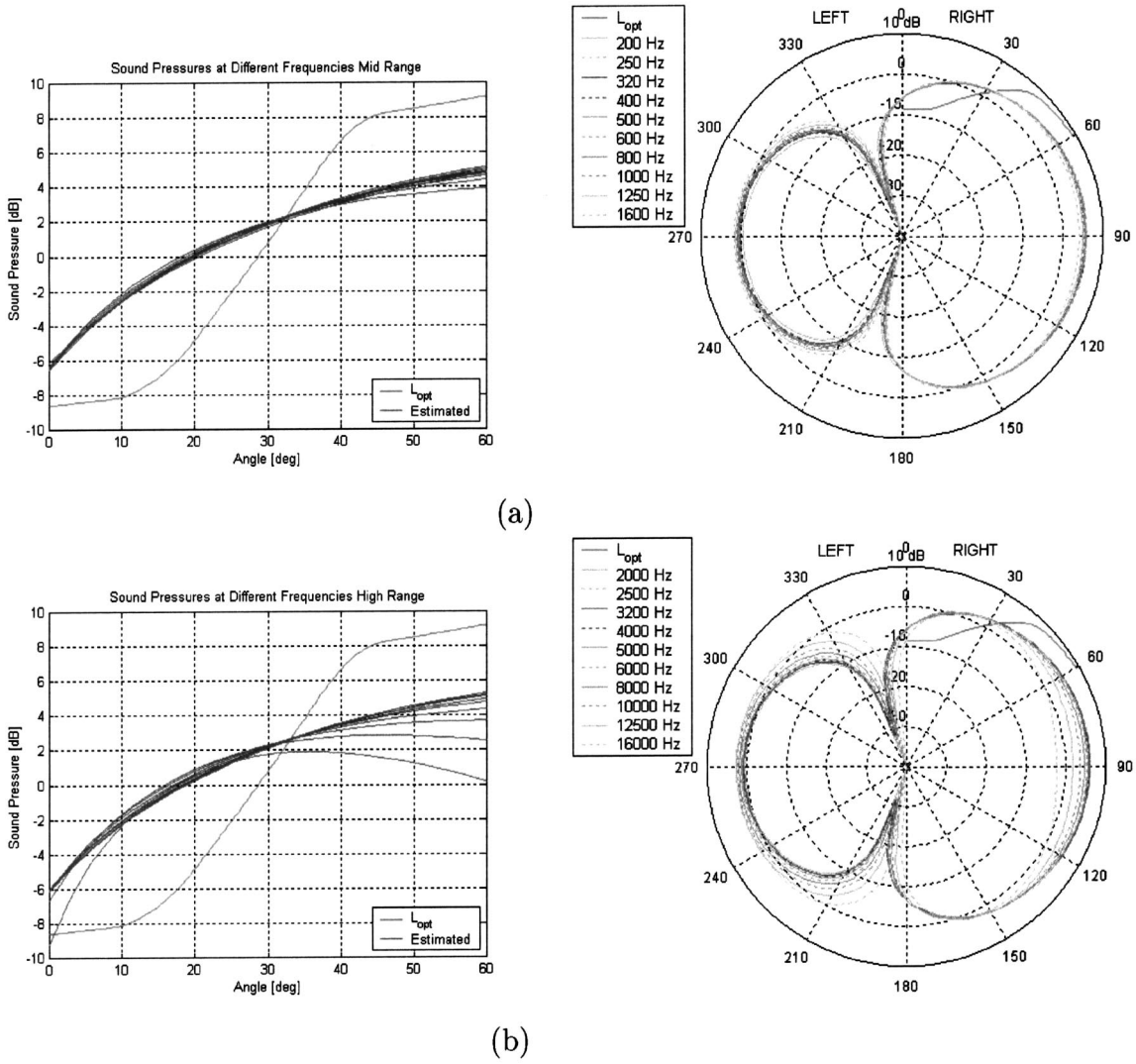

FIG. 12. Sound pressures and polar plots at different frequencies in the working region for the required FIR filters. (a) Midrange. (b) High range.

listening area has been presented. This optimal directivity pattern has been adapted to parametrized time/intensity trading data for enlarging the sweet spot area.

It has also been illustrated that imaging in the traditional stereophonic system is restricted to an extremely narrow listening area. Outside this area, spatial distortion of the sound image occurs.

A digital filtering technique for PI-stereo has been designed and applied to the individual drivers of loudspeaker arrays in a cabinet in order to achieve the optimal frequency-independent directivity pattern.

Preliminary listening tests have shown that the PI-stereo system, based on the optimal directivity pattern ℓ_{opt}, worked as predicted by the theoretical simulations. The system also demonstrated correct central sound localization for speech and music for a large listening area. PI-stereo images appear to be more robust with lateral movement than images in normal stereo. The stereo sound sensation was listening-position independent, thus enlarging the sweet spot area.

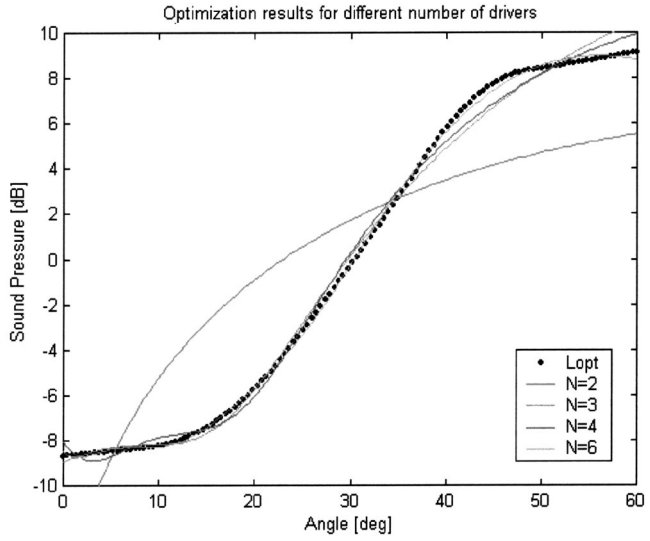

FIG. 13. Optimization results for the approximation of the ℓ_{opt} for different number of drivers N in the loudspeaker array.

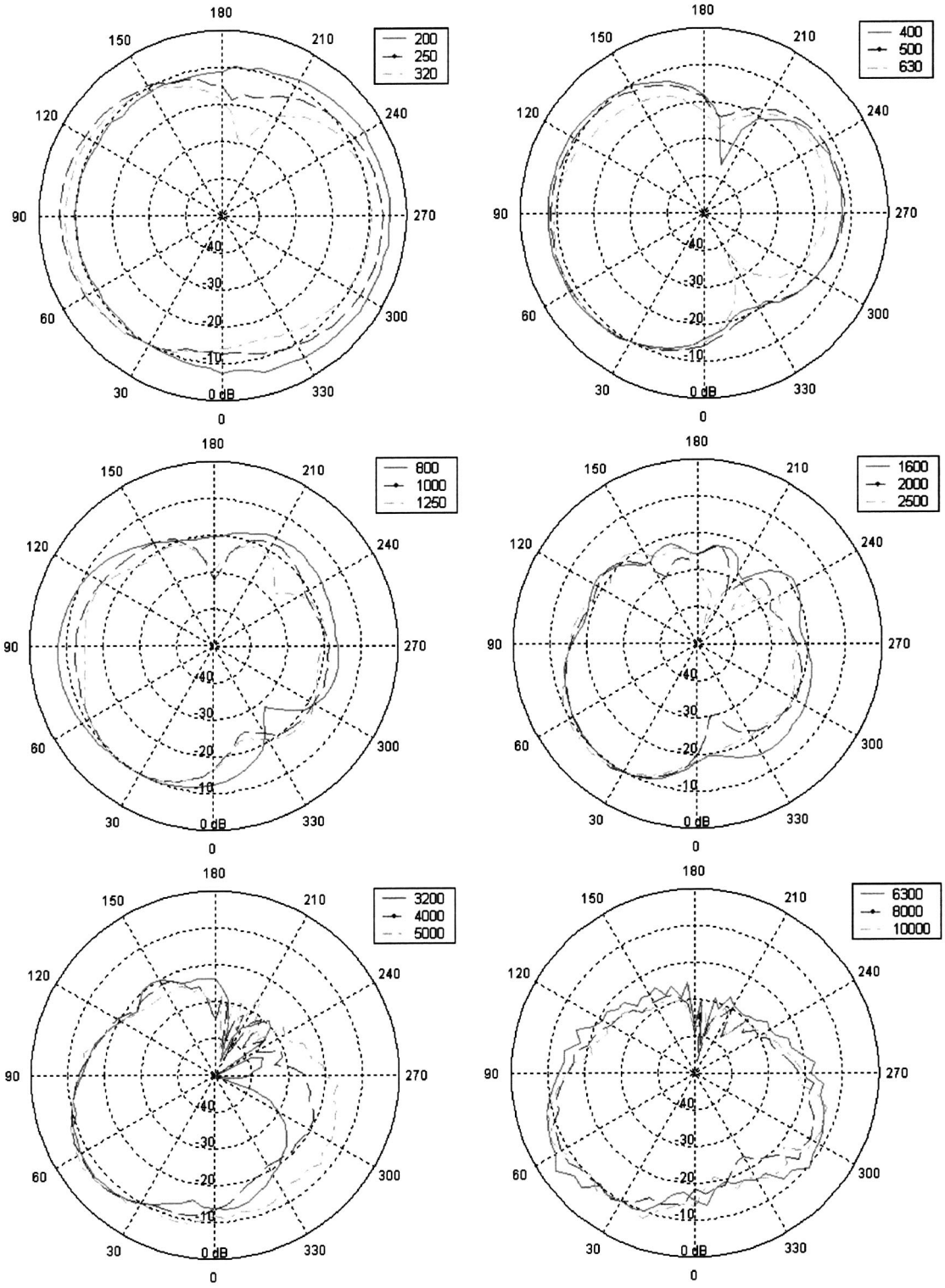

FIG. 14. Measured directivity pattern plots at different frequencies normalized at 30° for the right PI-stereo cabinet.

The outcome of this work has shown that an optimal directivity pattern for loudspeaker arrays in stereophonic applications can be very useful for sweet spot widening.

ACKNOWLEDGMENTS

The authors would like to thank Professor John Vanderkooy for his very valuable comments and suggestions for improving the final manuscript.

APPENDIX: OPTIMAL DIRECTIVITY PATTERN ℓ_{opt}

Given a function $h(\varphi,\psi)$ with $\varphi,\psi\in[0,\pi/2]$, satisfying Eq. (19), we seek to minimize

$$d_w^2(\ell(\varphi)-\ell(\psi)-h(\varphi,\psi)):$$

$$=\int_0^{\pi/2}\int_0^{\pi/2}|\ell(\varphi)-\ell(\psi)-h(\varphi,\psi)|^2 w(\varphi)w(\psi)d\varphi\, d\psi, \tag{A1}$$

over all square integrable functions $\ell(\varphi)$ (with respect to the weight $w(\varphi)$ with $\varphi\in[0,\pi/2]$), satisfying Eq. (24). In Eq. (A1) the weight function w is bounded and non-negative.

We consider the linear subspace M of all square integrable functions [with respect to the weight $w(\varphi)w(\psi)$ as in Eq. (A1)] of the form:

$$k(\varphi,\psi)=\ell(\varphi)-\ell(\psi),\quad \varphi,\psi\in\left[0,\frac{\pi}{2}\right] \tag{A2}$$

with ℓ satisfying Eq. (24). Furthermore, we let P_M be the orthogonal projection operator of the space of all square integrable functions $h(\varphi,\psi)$ satisfying $h(\psi,\varphi)=-h(\varphi,\psi)$ as in Eq. (19) onto the space M. Then, minimizing the functional in Eq. (A1) amounts to finding the orthogonal projection $P_M h$ of h as

$$(P_M h)(\varphi,\psi)=\ell_{\text{opt}}(\varphi)-\ell_{\text{opt}}(\psi),\quad \varphi,\psi\in\left[0,\frac{\pi}{2}\right], \tag{A3}$$

where $\ell=\ell_{\text{opt}}$ is square integrable [with respect to the weight $w(\varphi)$], satisfies Eq. (24), and minimizes Eq. (A1).

We compute for an ℓ as above

$$\begin{aligned}
&d_w^2(\ell(\varphi)-\ell(\psi)-h(\varphi,\psi))\\
&\quad=\int_0^{\pi/2}\int_0^{\pi/2}(|\ell(\varphi)|^2+|\ell(\psi)|^2\\
&\qquad-2\ell(\varphi)\ell(\psi))w(\varphi)w(\psi)d\varphi\ d\psi\\
&\qquad-2\int_0^{\pi/2}\int_0^{\pi/2}h(\varphi,\psi)\ell(\varphi)w(\varphi)w(\psi)d\varphi\ d\psi\\
&\qquad+2\int_0^{\pi/2}\int_0^{\pi/2}h(\varphi,\psi)\ell(\psi)w(\varphi)w(\psi)d\varphi\ d\psi\\
&\qquad+\int_0^{\pi/2}\int_0^{\pi/2}|h(\varphi,\psi)|^2w(\varphi)w(\psi)d\varphi\ d\psi.
\end{aligned} \tag{A4}$$

Now we have

$$\begin{aligned}
&\int_0^{\pi/2}\int_0^{\pi/2}|\ell(\varphi)|^2w(\varphi)w(\psi)d\varphi\ d\psi\\
&\quad=\int_0^{\pi/2}\int_0^{\pi/2}|\ell(\psi)|^2w(\varphi)w(\psi)d\varphi\ d\psi\\
&\quad=C\int_0^{\pi/2}|\ell(\varphi)|^2w(\varphi)d\varphi,
\end{aligned} \tag{A5}$$

where C is given by Eq. (26), and

$$\begin{aligned}
&\int_0^{\pi/2}\int_0^{\pi/2}\ell(\varphi)\ell(\psi)w(\varphi)w(\psi)d\varphi\ d\psi\\
&\quad=\left(\int_0^{\pi/2}\ell(\varphi)w(\varphi)d\varphi\right)^2=0
\end{aligned} \tag{A6}$$

by Eq. (24). Also, using Eqs. (19) and (24), we have

$$\begin{aligned}
&\int_0^{\pi/2}\int_0^{\pi/2}h(\varphi,\psi)\ell(\varphi)w(\varphi)w(\psi)d\varphi\ d\psi\\
&\quad=-\int_0^{\pi/2}\int_0^{\pi/2}h(\varphi,\psi)\ell(\psi)w(\varphi)w(\psi)d\varphi\ d\psi\\
&\quad=\int_0^{\pi/2}\ell(\varphi)m_w(\varphi)d\varphi,
\end{aligned} \tag{A7}$$

where we have set

$$m_w(\varphi)=\int_0^{\pi/2}h(\varphi,\psi)w(\psi)d\psi,\quad \varphi\in\left[0,\frac{\pi}{2}\right]. \tag{A8}$$

It follows that

$$\begin{aligned}
&d_w^2(\ell(\varphi)-\ell(\psi)-h(\varphi,\psi))\\
&\quad=2C\int_0^{\pi/2}\left(\ell(\varphi)-\frac{1}{C}m_w(\varphi)\right)^2w(\varphi)d\varphi\\
&\qquad+\int_0^{\pi/2}\int_0^{\pi/2}|h(\varphi,\psi)|^2w(\varphi)w(\psi)d\varphi\ d\psi\\
&\qquad-\frac{2}{C}\int_0^{\pi/2}m_w^2w(\varphi)d\varphi.
\end{aligned} \tag{A9}$$

Hence, the minimal value of the functional occurs for

$$\ell_{\text{opt}}(\varphi)=\frac{1}{C}m_w(\varphi),\quad \varphi\in\left[0,\frac{\pi}{2}\right], \tag{A10}$$

where C and m_w are given by Eqs. (26) and (A8). The function ℓ_{opt} is unique on the set of all φ with $w(\varphi)>0$.

In Sec. V B [Eq. (18)] we have h of the form

$$h(\varphi,\psi)=f\left(\frac{D\ \sin 1/2(\varphi-\psi)}{c\ \cos 1/2(\varphi+\psi)}\right),\quad \varphi,\psi\in\left[0,\frac{\pi}{2}\right] \tag{A11}$$

with $f(x)$ an odd, piecewise linear function of $x\in\mathbf{R}$. Such an h indeed satisfies Eq. (19). Furthermore, the integral representation of $m_w(\varphi)$, as needed in Eq. (A10) for ℓ_{opt}, can be rewritten by introducing for any $\varphi\in[0,\pi/2]$ the new variable

$$\begin{aligned}
x&=\frac{\sin 1/2(\varphi-\psi)}{\cos 1/2(\varphi+\psi)}\\
&=\sin\varphi-\cos\varphi\ \tan\tfrac{1}{2}(\varphi+\psi)\in[-1,\tan\tfrac{1}{2}\varphi].
\end{aligned} \tag{A12}$$

Solving ψ from Eq. (A12) [which is most easily done by using the second right-hand side member in Eq. (A12)], we find

$$\psi=\varphi-2\arctan\left(\frac{x\ \cos\varphi}{1-x\ \sin\varphi}\right), \tag{A13}$$

and

$$d\psi=\frac{-2\cos\varphi}{1-2x\ \sin\varphi+x^2}dx. \tag{A14}$$

This then yields Eq. (27).

Aarts, R. M. (**1992**). ''Time/intensity trading stereophony for (HD)TV and audio applications,'' in *14th International Congress on Acoustics* (Beijing, China) (session L8-3).
Bauer, B. B. (**1960**). ''Broadening the area of stereophonic perception,'' J. Audio Eng. Soc. **8**, 91–94.
Blauert, J. (**1983**). *Spatial Hearing* (MIT Press, Cambridge, MA).
Blumlein, A. D. (**1958**). ''Improvements in and relating to sound-transmission, sound-recording, and sound-reproducing systems,'' J. Audio Eng. Soc. **6**, 91–98.
Crabbe, J. (**1979**). ''Broadening the stereo seat,'' HI-FI News Record Rev. **24**, 64–68.
Davis, M. F. (**1987**). ''Loudspeaker systems with optimized wide-listening area imaging,'' J. Audio Eng. Soc. **35**, 888–896.
Dennis, J. E. (**1977**). *Nonlinear Least Squares: State of the Art in Numerical Analysis* (Academic, New York).
Franssen, N. V. (**1960**). ''Some Considerations on the Mechanism of Directional Hearing,'' Ph.D. thesis, Technical University of Delft, The Netherlands.
Jordan, E. J. (**1971**). ''Loudspeaker stereo techniques: How to combine left and right signals and get the message from the medium,'' Wireless World, 67–70.
Kates, J. (**1980**). ''Optimum loudspeaker directional patterns,'' J. Audio Eng. Soc. **28**, 787–794.
Leakey, D. M. (**1959**). ''Some measurements on the effects of interchannel intensity and time differences in two channel sound systems,'' J. Acoust. Soc. Am. **31**, 977–986.
Leakey, D. M. (**1960**). ''Further thoughts on stereophonic sound systems,'' Wireless World, 154–160.
Lipshitz, S. P. (**1986**). ''Stereo microphone techniques,'' J. Audio Eng. Soc. **34**, 716–744.
Makita, Y. (**1962**). ''The directional localization of sound in the stereophonic sound field,'' E.B.U. Review **73**, 102–108.
Marquardt, D. (**1963**). ''An algorithm for least-squares estimation of nonlinear parameters,'' SIAM (Soc. Ind. Appl. Math.) J. Appl. Math. **11**, 431–441.
Rodenas, J. A., and Aarts, R. M. (**2001a**). ''Position independent stereophonic sound reproduction,'' Nederlands Akoestisch Genootschap NAG Journal, 37–47.
Rodenas, J. A., and Aarts, R. M. (**2001b**). ''Sweet spot widening for stereophonic sound reproduction,'' in *IEEE WASPAA*, New Paltz, NY, 21–24 October, pp. 191–194.
Stevens, S. S., and Newman, E. B. (**1936**). ''The localization of actual sources of sound,'' Am. J. Psychol. **48**, 297–306.